X-621-70-320
PREPRINT

NASA TM X-65321

ION AND NEUTRAL COMPOSITION CHANGES IN THE THERMOSPHERIC REGION DURING MAGNETIC STORMS

S. CHANDRA
P. STUBBE

AUGUST 1970

GSFC

GODDARD SPACE FLIGHT CENTER
GREENBELT, MARYLAND

ION AND NEUTRAL COMPOSITION CHANGES IN THE THERMOSPHERIC REGION DURING MAGNETIC STORMS

by

S. Chandra
Thermosphere & Exosphere Branch
Laboratory for Planetary Atmospheres
Goddard Space Flight Center, Greenbelt, Maryland 20771

and

P. Stubbe
Max-Planck - Institut für Aeronomie
3411 Lindau / Harz, West Germany

ABSTRACT

The structural differences of the ion and neutral composition in the thermospheric region are studied by solving a system of basic ionospheric and atmospheric equations. The study shows that the compositional changes during a magnetic storm arise largely as a result of changes in the neutral composition at the turbopause. A decrease in $[O]/[N_2]$ in the lower atmosphere triggers a complex chain of events which results in an increase of the neutral gas temperature, depletion of the O^+ layer and enhancement of NO^+. The relative changes in these layers occasionally produce a sequence of electron density profiles giving rise to the so-called G condition. It is shown that, compared to the neutral atmosphere, the ionosphere is much more sensitive to the changes in $[O]/[N_2]$ in the lower thermospheric region. Since the ionospheric parameters can be measured much more accurately than the atmospheric parameters, it is argued that they should form an integral part of the observational data required to construct the atmospheric models.

1. INTRODUCTION

It has been recognized for some time that the ionospheric effects associated with geomagnetic disturbances are principally the result of changes in the neutral composition of the upper atmosphere (King, 1962, 1966, 1967; Duncan, 1969). This assumption has generally been invoked to explain the changes in the F-region critical frequencies (f_oF_2) observed during the storm period. Since direct measurements of the neutral composition during geomagnetic disturbances are almost non existent, the validity of this concept could not be tested beyond its ability to explain the observed increase or decrease in f_oF_2. In recent years electron density and temperature measurements from satellites and incoherent radar backscatter during magnetic storms have extended our horizon beyond the height of the F-region maximum (King et al., 1967; Bauer and Krishnamurthy, 1968; Norton, 1969; Reddy et al., 1967, 1969; Evans, 1965; Rao, 1968). Although these observations are only few, they provide a much wider base for testing the concept of neutral composition changes during geomagnetic storms. In addition, a number of important papers have appeared in recent years describing the behavior of airglow in the various wave length bands during magnetic storms (Weil and Glaume, 1967; Truttse, 1968). These measurements provide direct evidence to the changes in the neutral composition (Krassovsky, 1968) and thus offer an excellent opportunity for studying the behavior of the neutral atmosphere during storm periods.

The physical mechanisms causing variations in the neutral atmosphere during storms are not fully understood. Cole (1962, 1965) has proposed two principal mechanisms by which energy is deposited in the upper atmosphere during magnetic storms. These are: (1) the thermal conduction of the energy from the magnetosphere to the ionosphere and; (2) the Joule dissipation of the ionospheric currents. The two mechanisms are complementary and not mutually exclusive. They are responsible for a deposition of energy in different regions of the upper atmosphere. Since Joule heating occurs principally in the auroral regions, the transfer of energy to the lower latitudes probably occurs by gravity waves (Hines, 1965). Cummings and Dessler (1967) propose Joule dissipation of the asymmetric ring current as an alternative mechanism for the deposition of energy in the auroral and subauroral region of the lower atmosphere. Regardless of the merit of any particular mechanism, it is reasonable to believe that the energy deposited in the altitude range around 120 km should cause a change in the circulation pattern of the lower atmosphere resulting in the change of the turbopause level and the neutral compositon of that region. This is the basic assumption of this paper. Its justification lies in its ability to explain the storm related changes in the upper atmosphere.

Any change in the composition of the neutral atmosphere not only affects the structural parameters of the region where the change takes place but also affects the other regions profoundly through a series of complex processes involving diffusion, transport and heat conduction. Thus, in order to understand the changes in the upper atmosphere, it is important to consider the behavior of the neutral and ionized constituents as one problem. This point was clearly established in a recent paper by Chandra and Herman (1969). Through simultaneous steady state solutions of the electron continuity equation and the heat conduction equations for electrons, ions and the neutral gas, the authors showed how some of the well known features of the F-region storm can be explained by assuming a decrease in the ratio of atomic oxygen to molecular nitrogen, $[O]/[N_2]$, at the lower boundary. Such an assumption was consistent with the storm-time increase in the neutral density inferred from satellite drag observations.

The purpose of this paper is to present detailed time dependent calculations of the changes in composition of both the ionized and neutral constituents of the upper atmosphere resulting from the changes in the relative values of $[O]$, $[O_2]$ and $[N_2]$ at the lower boundary. The results are discussed in terms of the observed changes during geomagnetic storms.

2. FUNDAMENTAL EQUATIONS

The results of this paper are based on the simultaneous solution of a system of coupled, time dependent differential equations consisting of:

1. Equations of continuity for O^+, NO^+, and H^+
2. Heat conduction equations for O^+, H^+ and the electron and neutral gas.
3. Equations of motion of the various ionic and neutral constituents.

These equations and their method of solution have been fully described by Stubbe (1970) and will not be repeated here. The neutral atmosphere is assumed to consist of O_2, N_2, O, H and He. Their height variaions are described by Chandra and Stubbe (1970) in terms of the dynamic diffusion model. The dynamic diffusion model was introduced in order to account for the observed phase difference between the neutral density as derived from satellite drag data and the neutral temperature as derived from incoherent backscatter.

All the calculations are performed for a mid-latitude station (Geographic latitude 42°; dip angle 72°), roughly corresponding to Millstone, at equinox. The solar flux is assumed to be 30% higher than that given by Hinteregger et al.(1965), corresponding to low to medium solar activity. Following the convention of Chandra and Herman, we have characterized the assumed values of [O], [O_2], [N_2] and T_N at the lower boundary (120 km) by quiet and disturbed conditions. Their values at 120 km for 1800 hours local time are given in the following table.

	QUIET (Q)	DISTURBED (D_1)	DISTURBED (D_2)
O_2	$1.13 \times 10^{11}/cm^3$	$1.13 \times 10^{11}/cm^3$	$1.69 \times 10^{11}/cm^3$
N_2	$6.00 \times 10^{11}/cm^3$	$6.00 \times 10^{11}/cm^3$	$9.00 \times 10^{11}/cm^3$
O	$6.76 \times 10^{10}/cm^3$	$3.80 \times 10^{10}/cm^3$	$5.00 \times 10^{10}/cm^3$
T_N	355°K	355°K	355°K

The time variations in density at 120 km are assumed to be of the form $(1+0.3 \cos\omega t)$, and the temperature is assumed to vary as $(1+0.1 \cos\omega t)$ where ω is the angular frequency of the earth's rotation and t the time measured from noon. Note that the difference between D_1 and Q is only with respect to the values of [O]. In D_1, the [O] concentration is assumed to be about 50% less than in Q. In D_2, [O] is 25% less than in Q, while [O_2] and [N_2]

are assumed to be increased by 50%.

The composition changes from Q to D_1 and D_2 conditions assumed in this paper are arbitrary and are meant for illustration only. The observational data on the neutral composition in the lower atmosphere is still scarce. The difference between the various measurements is so large that it is difficult to construct models for quiet conditions, much less for disturbed conditions. The tasks of making quantitative estimates for composition changes during the period of geomagnetic storms is even more formidable. The altitude of the turbopause level and its variation during magnetic storms are the key parameters which must be calculated to compute the changes in the neutral composition at a specified reference level. This requires not only the knowledge of the source of energy and its magnitude but also the mechanism for its dissipation before the system of dynamical and energy equations can be solved for this purpose. Evidence has recently been presented (Testud and Vasseur 1970) that the energy generated in the auroral thermosphere during magnetic storms can be carried to the lower latitudes via gravity waves. The attempts to show how this can affect the composition changes in the lower atmosphere have not been successful. In view of these difficulties it is reasonable to make specific assumptions about the composition changes at the lower boundary and study their affects on the structural parameters of the neutral and ionized gas in the thermospheric region. The validity of these assumptions may then be tested by comparing the theoretical calculations with the observational data. This is the approach adopted in this paper.

Discussion of the Results

The Figures la and lb show the diurnal variations in N_mF_2 and the total electron content n_t (integrated from 120 to 1000 km) for the three conditions Q, D_1 and D_2. The corresponding variations in the neutral density at 200 km and the exospheric neutral temperature are shown in Figures 2a and 2b. The general inferences which can be drawn from these plots are as follows:

1. With the boundary conditions specified in Table 1, both N_mF_2 and n_t have decreased for the D_1 and D_2 conditions, compared to the Q condition. The decrease in N_mF_2 (about 40%) is comparatively larger than the corresponding decrease in n_t (about 20%). A slight discontinuity in N_mF_2 is caused by the development of the G condition to be discussed later.

2. Both the neutral density and the exospheric temperature T_∞ have increased considerably during the D_2 condition. On the other hand the increase in the exospheric temperature during the D_1 condition is rather small and the density in fact is slightly lower than for the Q condition.

It is important to note that T_∞ and ρ at 200 km for the Q and D_1 conditions are substantially the same and are considerably different from the D_2 condition. Nonetheless the N_mF_2 and n_t values for the D_1 and D_2 conditions are about the same and are quite different from N_mF_2 and n_t for the Q condition.

These results merely point towards the difficulty of constructing ionospheric and atmospheric models based only on the neutral density as inferred from satellite drag measurements. If the density shown in Figure 2a would have been measured by satellite drag, the result would have been that the Q and D_1 measurements refer to about the same atmospheric conditions, while the D_1 and D_2 measurements refer to different atmospheric conditions. The conclusion then would have been (since all the other parameters are assumed to be equal) that the ionospheres corresponding to Q and D_1 are the same and are different from the ionosphere corresponding to D_2. As we see here, just the opposite is the case. This indicates that the total neutral density does not give enough information to be the basis of atmospheric models. These points will be elaborated further in other examples.

The ion composition in the altitude range of 120 - 400 km for the three cases (Q, D_1 and D_2) is shown in Figures 3-5. Each figure gives the altitude profile of O^+, O_2^+, NO^+ along with the total electron density (sum of O^+, O_2^+, NO^+ and H^+) for 9.00, 12.00 and 15.00 hours local time on a linear scale. Figure 3 illustrates the development of the normal ionospheric layers F_1 and F_2 during the day. The electron density N_e near the F_2 peak gradually increases towards the afternoon as a result of the increase in O^+. The formation of the F_1 layer is almost entirely determined by NO^+ which attains its maximum values near noon. From Figures 4 and 5 which in our calculations represent stormtime conditions, we note that the O^+ layer is considerably depressed, causing a depression in the electron density near the F_2 peak.

The development of the various ionic layers over the day during the D_1 and D_2 conditions produces a rather interesting sequence of electron density profiles. With a single F layer in the morning hours to two layers (F_1 and F_2) in the noon and afternoon hours, it shows the development of a pattern which has been commonly known as a G condition during magnetic storms. The G condition results from a situation in which the critical frequency of the F_2-layer falls below that of F_1. A ground based ionosonde in this case records only the reflection from the F_1-layer. The situation is quite reversed when "seen" from the topside ionosphere. The ionogram in this case will show both F_1 and F_2 traces - a situation never encountered in the normal condition. A study of the G condition from topside ionograms has recently been made by Herzberg et al. (1969) and Fatkullin (1970). The calculations presented in Figures 4 and 5 illustrate the physical situation for the development of the G condition and the recovery from it.

The changes in ion composition during disturbed conditions in the altitude range below 300 km are not known experimentally. The results presented here show that the most pronounced effect occurs in the O^+ layer which is depleted considerably during storm conditions. This is accompanied by an increase in the NO^+ concentration, resulting in a slight increase in electron density near the F_1-peak. This is shown in Figure 6 where the ion composition for the Q and D_2 conditions is presented for 15:00 hours. The D_1 condition is not significantly different from D_2 and has been omitted in Figure 6 for clarity.

Figure 7 shows the altitude profiles of the neutral density and the ratio of [O] to [N_2] for the three cases Q, D_1 and D_2 corresponding to 15:00 hours. The exospheric temperatures T_∞ for the three cases as obtained from the solution of the heat conduction equation are also shown appropriately. It should be emphasized here again that all the parameters for the three cases are identical except for the differences in the assumed values of [O], [O_2] and [N_2] at the lower boundary. The D_1 and Q conditions which differ only with respect to the atomic oxygen density at 120 km show no significant change in the neutral density up to 300 km. The difference in the exospheric temperature is only about 40°K. The ionospheric models constructed from the two conditions, however, are significantly different. The comparison of D_1 and D_2 presents the opposite situation. The two cases lead to completely different atmospheres. Their exospheric temperatures are respectively 1084 and 1183°K. However, the ionospheric models constructed from these two cases are very similar. The understanding of this apparent dilemma is obtained by comparing the altitude profiles of $[O]/[N_2]$ for the three cases. We note from Figure 7 that at any given altitude $[O]/[N_2]$ is much larger for Q than for D_1 or D_2.

The series of events which follow a change in $[O]/[N_2]$ at the lower boundary is very complicated to describe. A certain insight, however, can be obtained from the following discussion: The main source of the thermal energy, responsible for heating the neutral atmosphere, is provided by the solar ultraviolet radiation. The U.V. is absorbed by the neutral constituents of the lower atmosphere, consisting mainly of atomic and molecular oxygen and molecular nitrogen. For a given U.V. flux the generation of thermal energy depends only on the relative concentration of O_2, N_2 and O. Out of these three constituents atomic oxygen also acts as a heat sink losing energy via infrared radiation. Since the maximum thermal energy is generated in the altitude range around 120 km where N_2 is the dominant constituent, the increase in $[N_2]$ and (or) decrease in $[O]$ results in a net increase of the thermal energy. This gives rise to a corresponding increase in the thermospheric temperature which, due to heat conduction, extends to high altitudes. The three neutral constituents O, N_2 and O_2, through rapid diffusion, almost instantaneously attain a new diffusive equilibrium distribution, corresponding to this increase in temperature. The net result then is an increase in O_2 and N_2 throughout the altitude region under consideration. In the case of O this increase is reflected only in the high altitude region. A larger value of $[N_2]$ and $[O_2]$ and a smaller value of [O] results in less production and more loss for O^+ causing depletion of this layer. Since NO^+ is produced at the expense of O^+, an increase in the loss rate for O^+ will cause an increase in NO^+.

SUMMARY AND CONCLUSION

Through the simultaneous solutions of a system of basic ionospheric and atmospheric equations we were able to simulate many of the observed features of the ionosphere for quiet and disturbed conditions. The main findings of this paper can be summarized as follows:

1. A decrease in $[O]/[N_2]$ at the lower boundary (120 km), arising from the decrease of the turbopause level during a magnetic storm, triggers a complex series of events resulting in the depletion of the O^+ layer and enhancement of NO^+. The development of these layers during the day can occasionally produce an interesting sequence of electron density profiles giving rise to the so called G condition.

2. The ionospheric parameters are much more sensitive to changes in $[O]/[N_2]$ than to changes in the absolute values of [O] and $[N_2]$. In the case of the neutral density, the situation is reversed. Since the ionospheric parameters can be measured much more accurately than the atmospheric parameters, it is very useful to consider their properties in constructing the atmospheric models.

3. Because of the variability of the turbopause level during a magnetic storm, it is not possible to compute the neutral temperature from the density measurements alone. The temperatures derived on the assumption of the invariant boundary cannot be considered to be a measure of the gas temperature and as such have very little physical significance.

The examples we chose in this paper to describe the stormtime behavior of the ionsophere correspond to what is generally called the negative phase of the storm, a phenomenon more common in middle and high latitudes. In low latitudes, the storm is generally accompanied by an increase in f_oF_2 giving rise to the positive phase. If the stormtime changes in the ionosphere are caused by the movement of the turbopause level, it is easy to visualize that the positive and negative phase of the storm result from the rise and fall of this le vel caused by the global circulation.

In this paper we limited our discussion to the changes in the neutral and ion compositions in the altitude range of 120 - 400 km. Even though the solutions of the heat conduction equations for electrons and ions (O^+, H^+) were an integral part of the solutions of the system of equations used in our study, we did not present any discussion on the behavior of electron and ion temperatures during magnetic storms. Our calculations showed that these temperatures increased during the D_1 and D_2 conditions following the pattern of the exospheric neutral temperatures. As we pointed out earlier in this paper, there are two principal mechanisms which are effective in depositing energy in the ionosphere during magnetic storms. These are: (1) The Joule dissipation of the ionospheric currents and; (2) the thermal conduction downward from the magnetosphere to the ionosphere along the geomagnetic field lines. In this paper we investigated only the consequences of the first mechanism. The second mechanism is responsible for heating the electron gas more efficiently, occasionally increasing its temperature to a point where it can give rise to a red arc condition through collisional excitation of atomic oxygen. Because of the general interest in the problem of the mid-latitude arc, the mechanism for heating the electron-ion gas merits a separate consideration. This will be the topic of a second paper. We should like to conclude this paper, however, with the statement that the ion and neutral composition changes discussed here arise primarily from the changes in the turbopause level. The increase in the electron and ion temperatures as a result of the downward conduction have practically no influence on the changes in ion and neutral composition below about 400 km.

ACKNOWLEDGEMENT

The work described in the present paper was carried out at the NASA-Goddard Space Flight Center and at the Max-Planck Institut für Aeronomie and is published with the permission of the Directors. One of us (S.C.) is thankful to Professor W. Dieminger for his kind invitation to work at the Max-Planck Institut für Aeronomie during this summer.

REFERENCES

Bauer, S.J., and B.V. Krishnamurthy (1968) Planet. Space Sci., 16, 653

Chandra, S., and J.R. Herman (1969) Planet. Space Sci., 17, 841

Chandra, S. and P. Stubbe (1970) Planet. Space Sci. 18

Cole, K.D. (1962) Australian J. Phys., 15, 223

Cole, K.D. (1965) J. Geophys. Res., 70, 1689

Cummings, W.D., and A.J. Dessler (1967) J. Geophys. Res., 72, 257

Duncan, R.A. (1969) J. Atmos. Terr. Phys., 31, 59

Evans, J.V. (1965) J. Geophys. Res., 70, 2726

Fatkullin, M.N. (1970) Geomag. & Aeronomy, 10 (3)

Herzberg, L., G.L. Nelms and P.L. Dyson (1969) Canadian J. Phys., 47, 2683

Hines, C.O. (1965) J. Geophys. Res., 70, 177

Hinteregger, H., L. Hall and G. Schmidtke (1965) Space Res., 5, 1175

King, J.W., K.C. Reed and E.C. Oiatunji (1967) J. Atmos. Terr. Phys., 29, 1355

King, G.A.M. (1962) Planet. Space Sci., 9, 95

King, G.A.M. (1966) J. Atmos. Terr. Phys., 28, 957

King, G.A.M. (1967) J. Atmos. Terr. Phys., 29, 161

Krassovsky, V.I.(1968) Annls. Geophys., 24, 1053

Norton, R.B. (1969) Proc. I.E.E.E., 57, 1147

Rao, P.B. (1968) J. Geophys. Res., 73, 1661

Reddy, B.M., L.H. Brace and J.A. Findlay (1967) J. Geophys. Res., 72, 2709

Reddy, B.M., D.R. Lakshami and L.H. Brace (1969) Radio Sci., 4, 851

Stubbe, P. (1970) J. Atmos. Terr. Phys., 32, 865

Testud, J., and G. Vasseur, Presented at the International Symposium on Waves in the Upper Atmosphere (Toronto, 19-22 January 1970).

Truttse, Y.L. (1968) Planet. Space Sci., 16, 981

Weill, G., and J.C. Glaume (1967) Annls. Geophys., 23. 317

FIGURE CAPTIONS

Figure 1a Diurnal variation of N_mF_2, the electron density at the F-peak, for the cases Q, D_1 and D_2.

Figure 1b Diurnal variation of the columnar electron content up to 1000 km for the cases Q, D_1 and D_2.

Figure 2a Diurnal variation of the neutral density at 200 km for the cases Q, D_1 and D_2

Figure 2b Diurnal variation of the exospheric neutral temperature for the cases Q, D_1 and D_2.

Figure 3 Changes in the ion composition during the day for the Q-case.

Figure 4 Changes in the ion composition during the day for the D_1-case, showing the development of a G-condition around noon.

Figure 5 Changes in the ion composition during the day for the D_2-case, showing the development of a G-condition around noon.

Figure 6 Comparison of the ion densities at 15 hours local time for the cases Q and D_2.

Figure 7 The neutral density and the ratio $[O]/[N_2]$ as a function of height at 15 hours local time for the cases Q, D_1 and D_2.

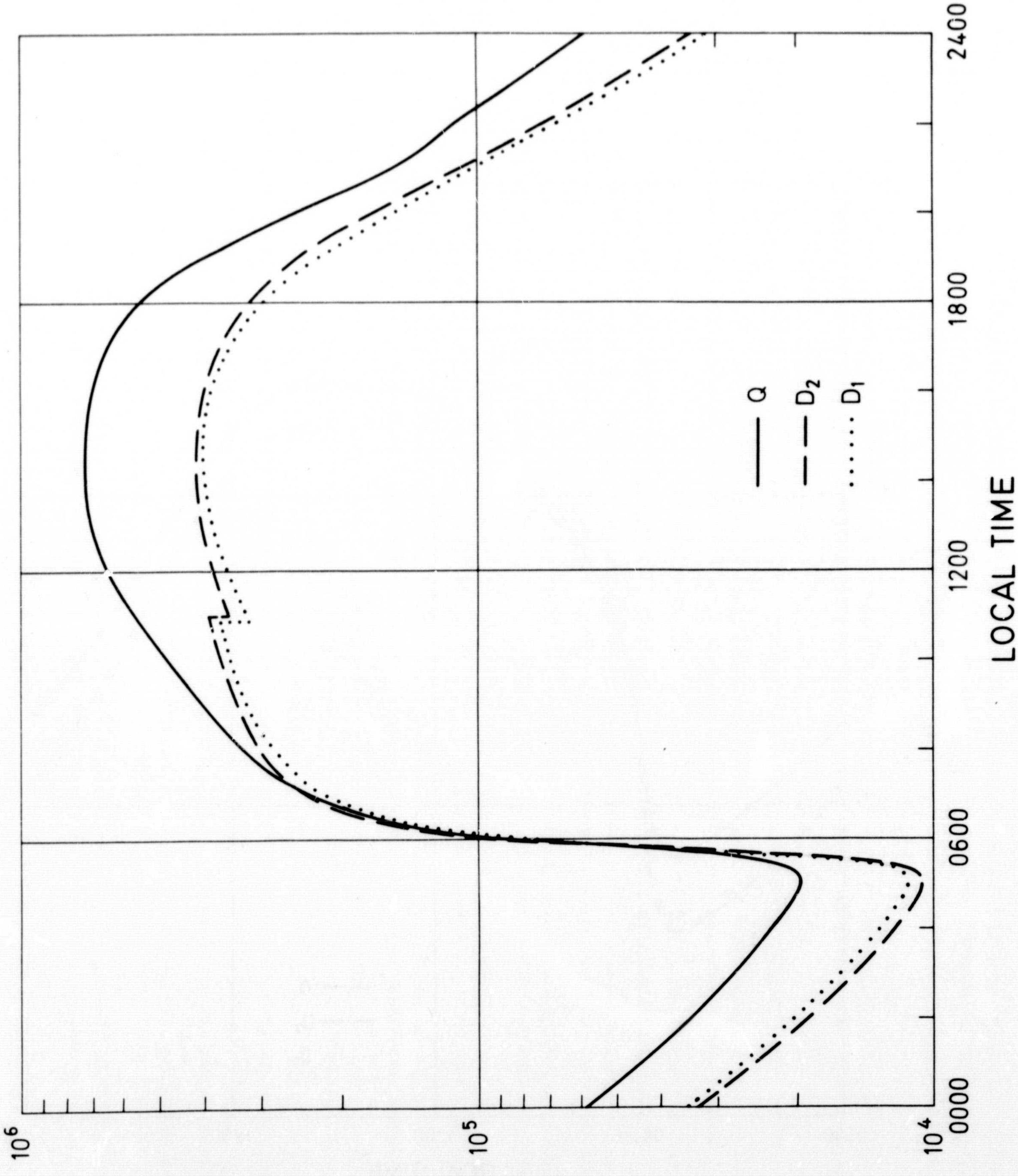

10^6
10^5
10^4
N_mF2 [CM^-3]
0000
0600
1200
1800
2400
LOCAL TIME
Q
D_2
D_1

Fig. 1a

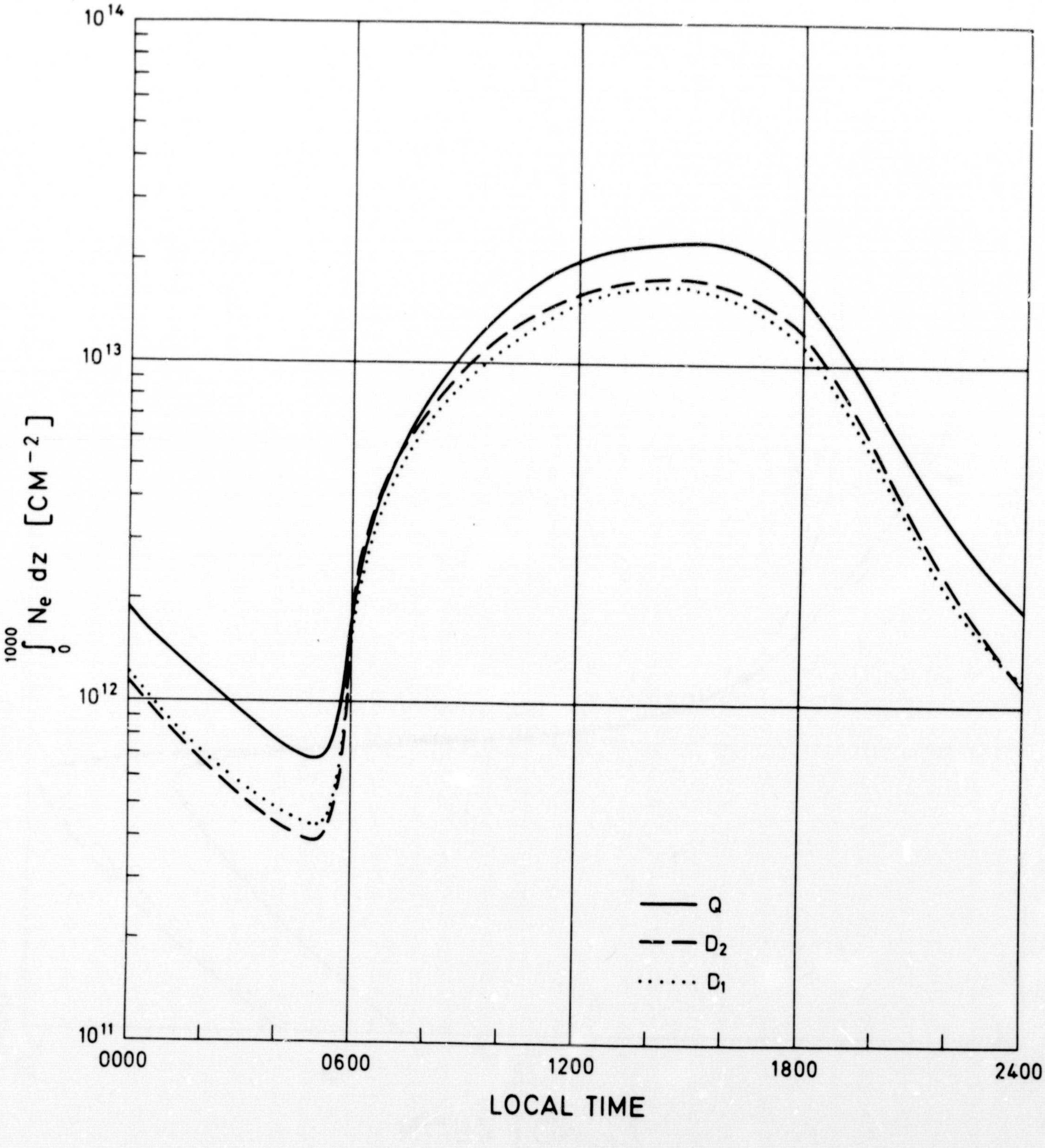

10^{14}
10^{13}
10^{12}
10^{11}
$\int_0^{1000} N_e \, dz$ [CM^{-2}]
0000
0600
1200
1800
2400
LOCAL TIME
Q
D_2
D_1

Fig. 1b

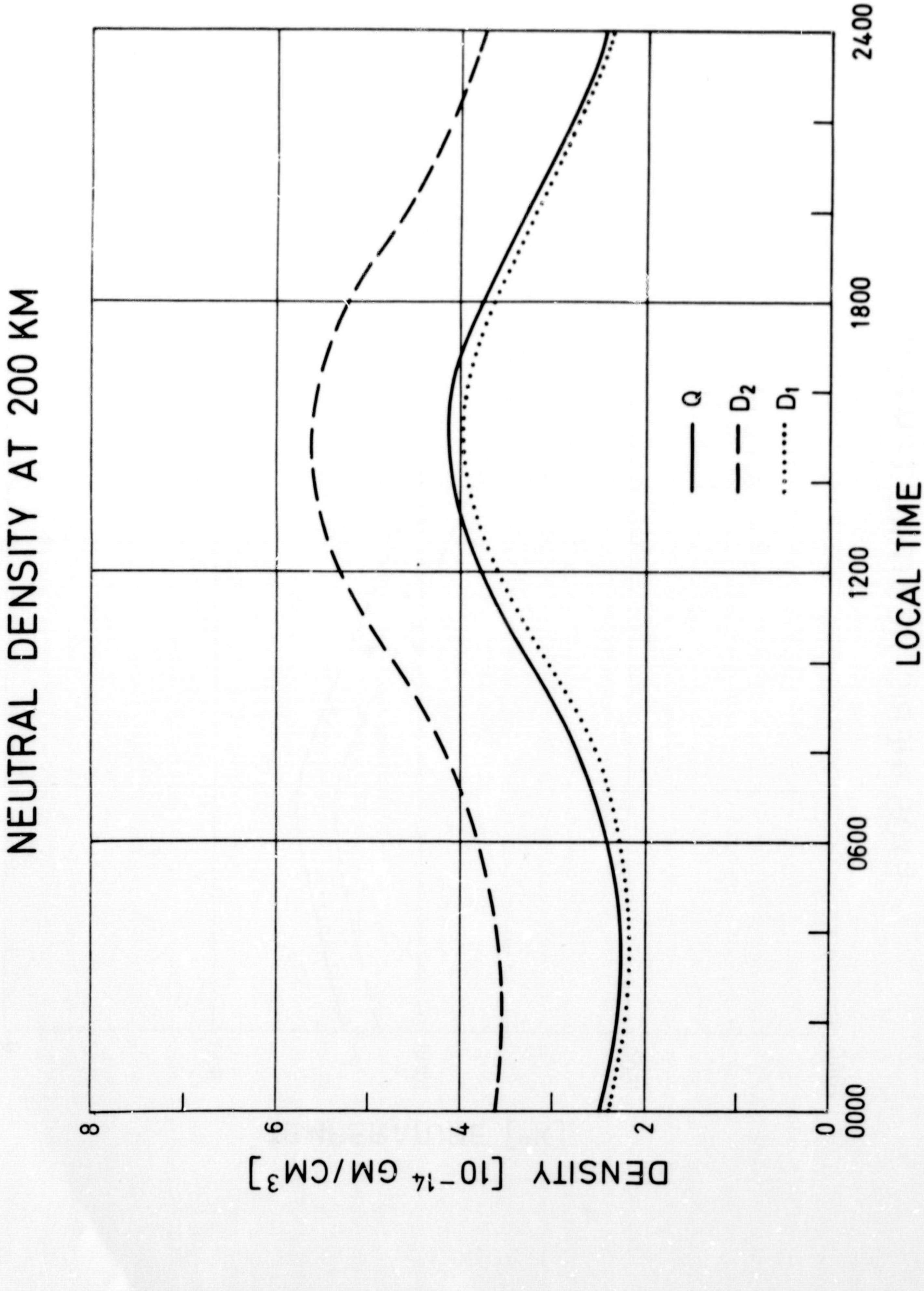
NEUTRAL DENSITY AT 200 KM
DENSITY [10^-14 GM/CM^3]
8
6
4
2
0
0000
0600
1200
1800
2400
LOCAL TIME
Q
D2
D1

Fig. 2a

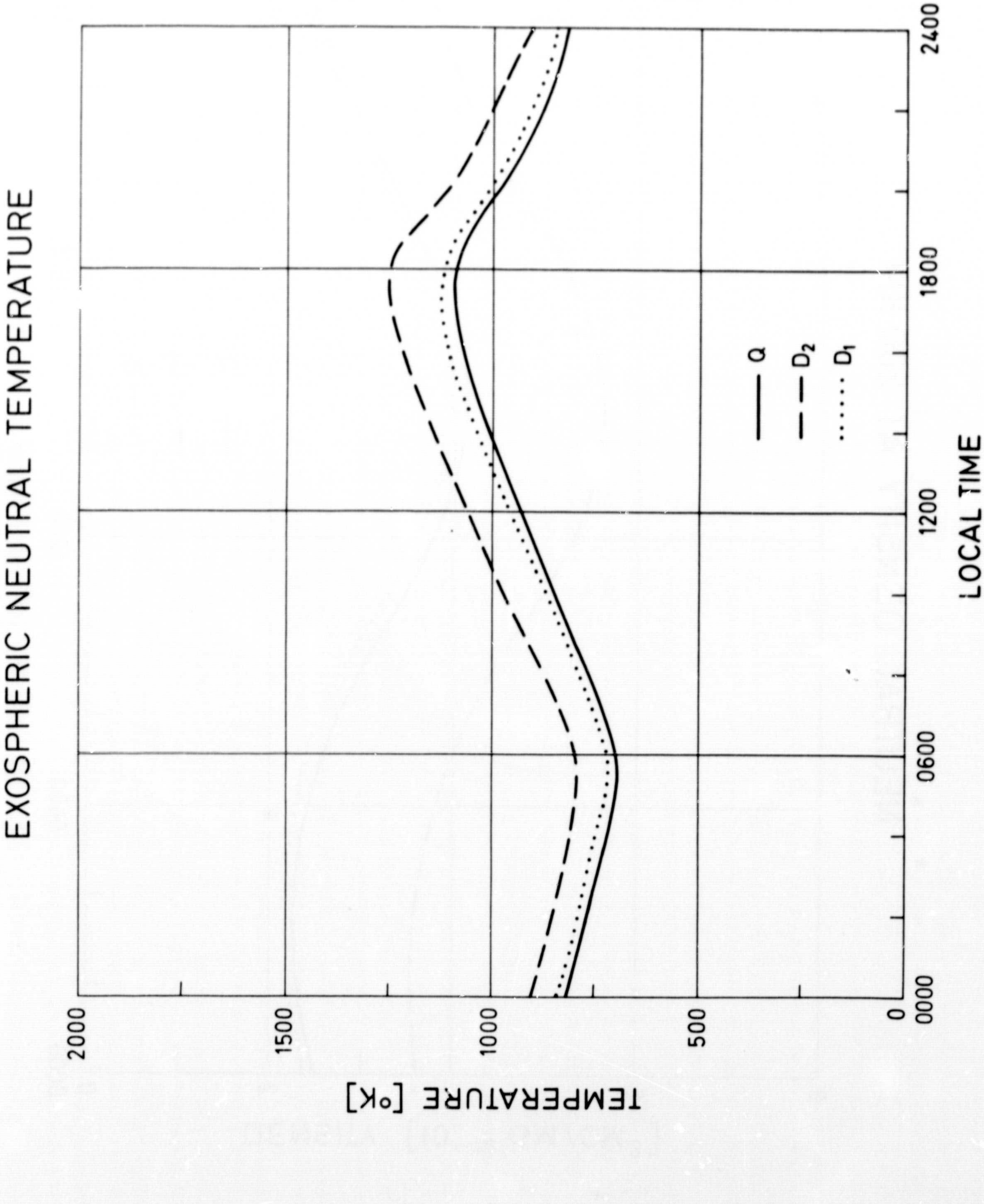
EXOSPHERIC NEUTRAL TEMPERATURE
TEMPERATURE [°K]
2000
1500
1000
500
0
0000
0600
1200
1800
2400
LOCAL TIME
Q
D2
D1

Fig. 2b

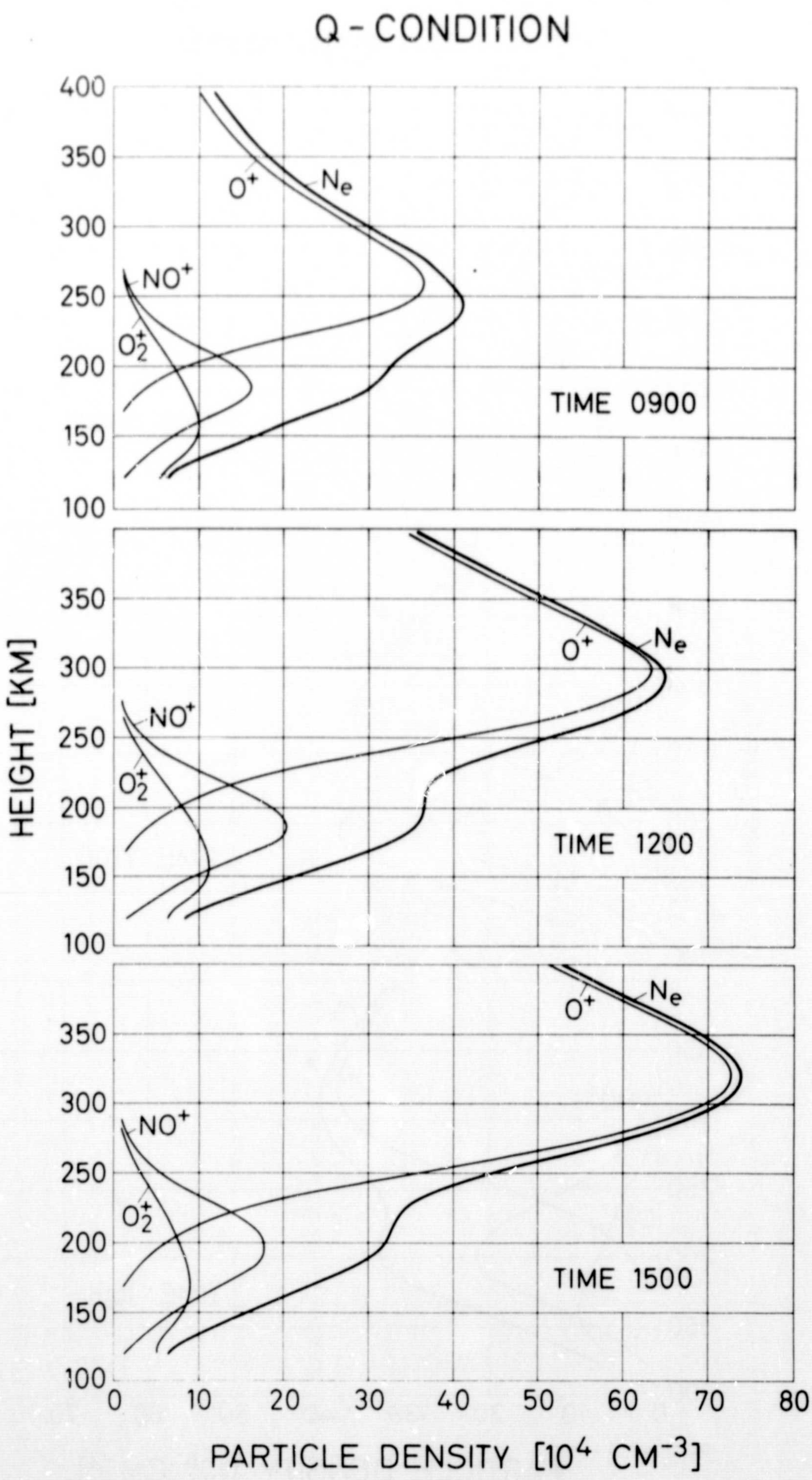

Q - CONDITION
HEIGHT [KM]
PARTICLE DENSITY [10^4 CM^{-3}]
TIME 0900
TIME 1200
TIME 1500
O^+
N_e
NO^+
O_2^+
100
150
200
250
300
350
400
0
10
20
30
40
50
60
70
80

Fig. 3

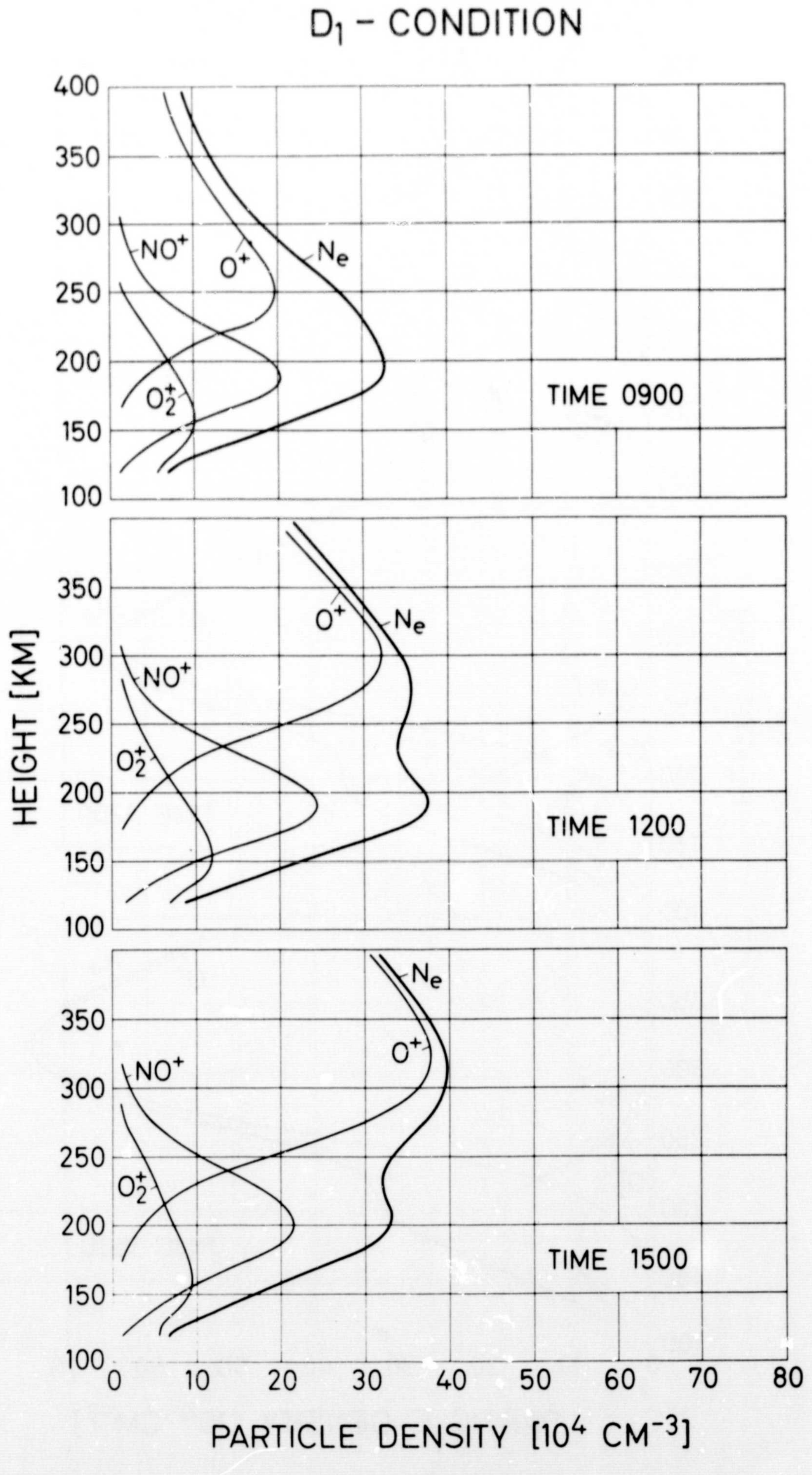

D1 - CONDITION
HEIGHT [KM]
PARTICLE DENSITY [10^4 CM^-3]
NO+
O+
Ne
O2+
TIME 0900
TIME 1200
TIME 1500
400
350
300
250
200
150
100
0
10
20
30
40
50
60
70
80

Fig. 4

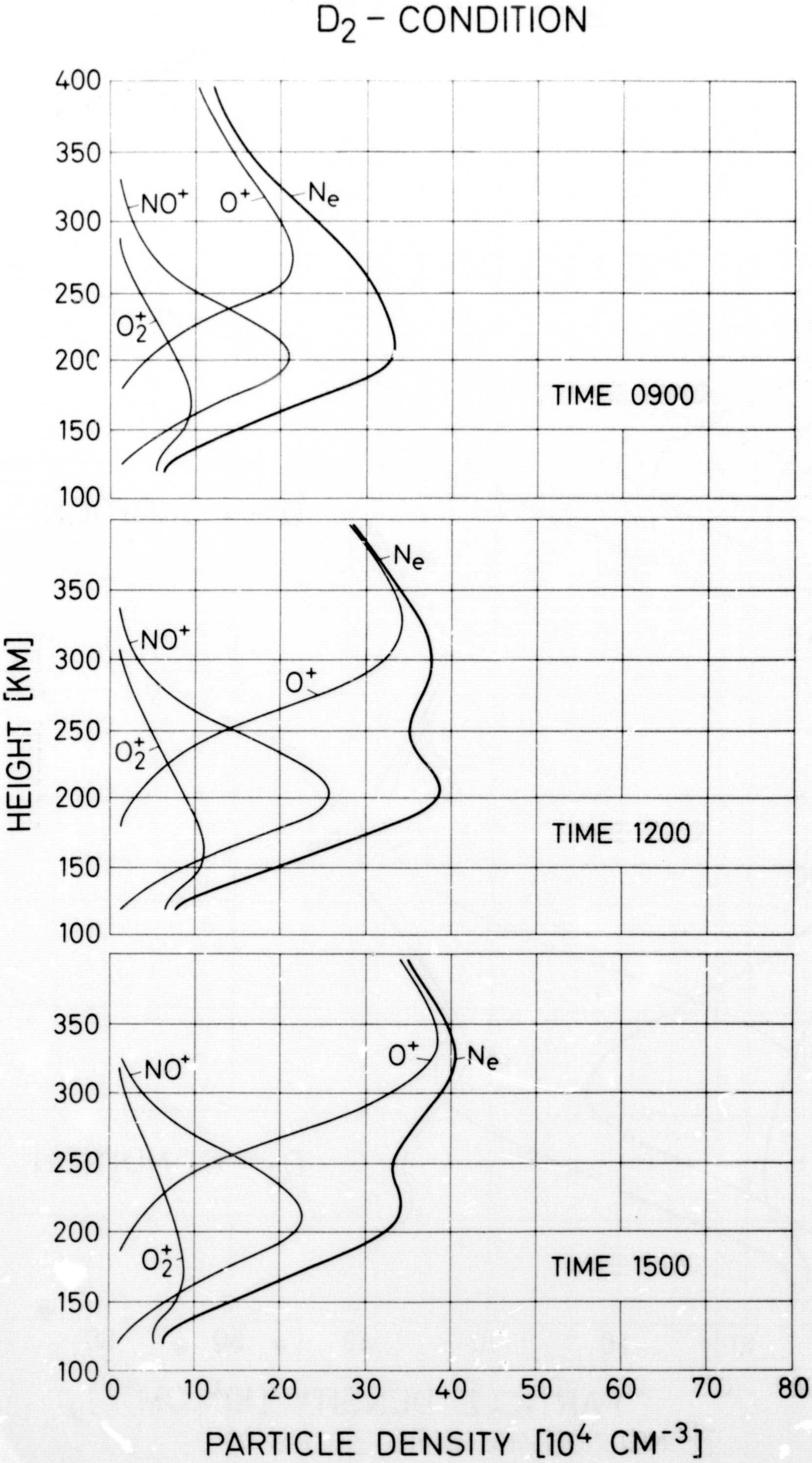

D2 - CONDITION
400
350
300
250
200
150
100
NO+
O+
Ne
O2+
TIME 0900
350
300
250
200
150
100
NO+
O+
Ne
O2+
TIME 1200
350
300
250
200
150
100
NO+
O+
Ne
O2+
TIME 1500
HEIGHT [KM]
0
10
20
30
40
50
60
70
80
PARTICLE DENSITY [10^4 CM^-3]

Fig. 5

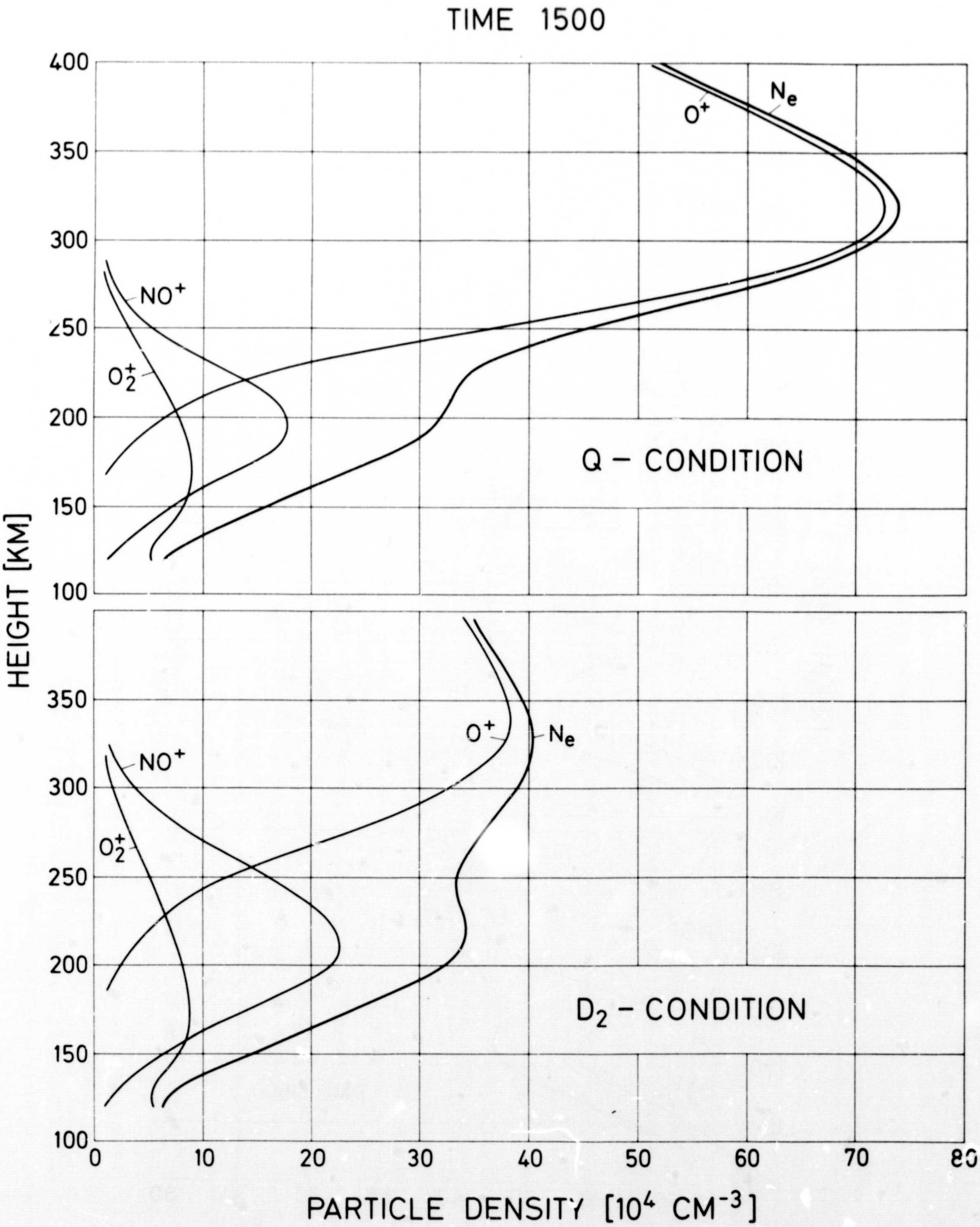
TIME 1500
HEIGHT [KM]
PARTICLE DENSITY [10^4 CM^{-3}]
O^+
N_e
NO^+
O_2^+
Q – CONDITION
D_2 – CONDITION
400
350
300
250
200
150
100
0
10
20
30
40
50
60
70
80

Fig. 6

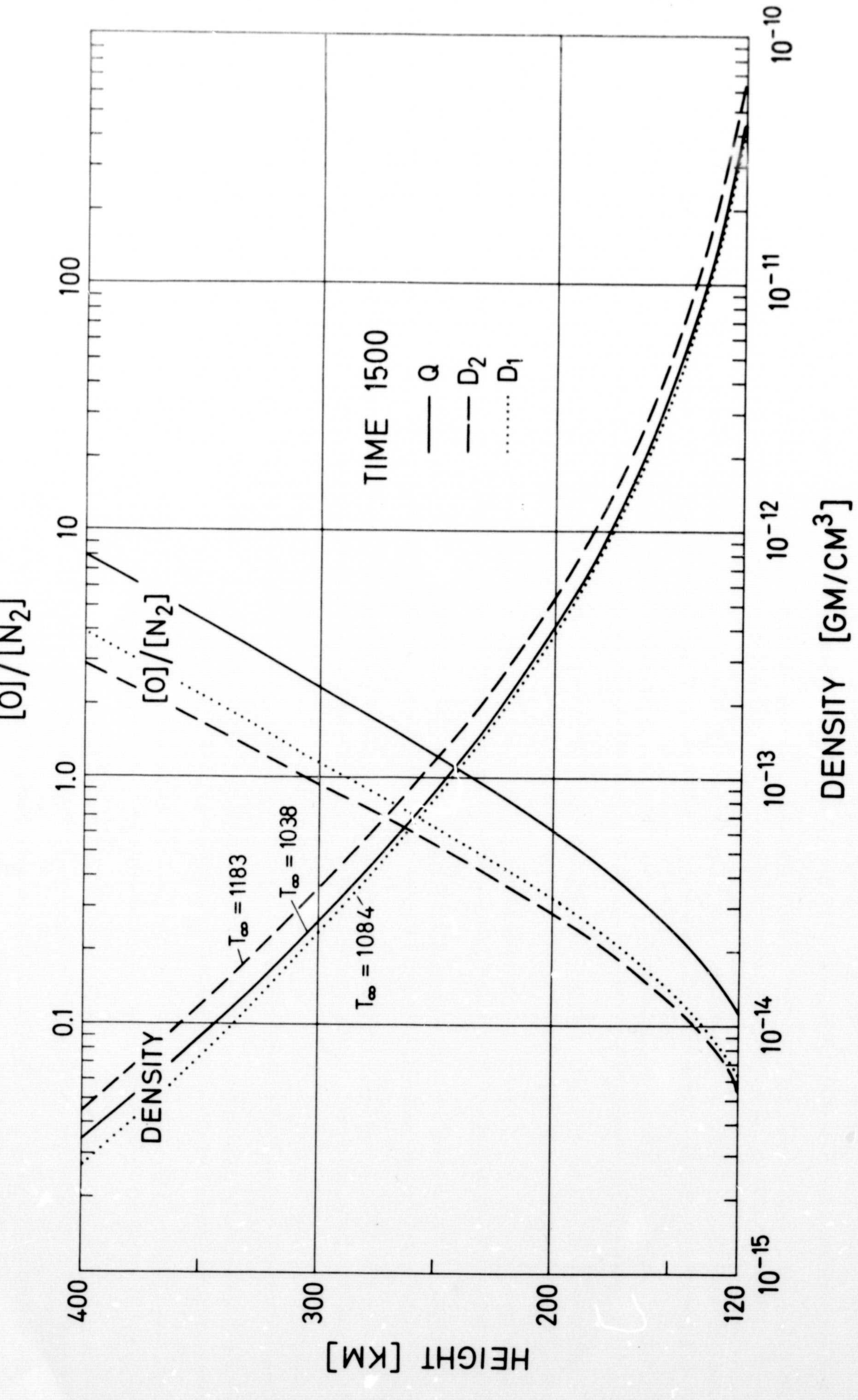

HEIGHT [KM]
400
300
200
120
[O]/[N2]
0.1
1.0
10
100
DENSITY [GM/CM3]
10-15
10-14
10-13
10-12
10-11
10-10
TIME 1500
Q
D2
D1
DENSITY
[O]/[N2]
T∞ = 1183
T∞ = 1038
T∞ = 1084

Fig. 7